Vaccine: X 14 (2023) 100347

Contents lists available at ScienceDirect

Vaccine: X

journal homepage: www.elsevier.com/locate/jvacx

Screening of apical membrane antigen-1 (AMA1), dense granule protein-7 (GRA7) and rhoptry protein-16 (ROP16) antigens for a potential vaccine candidate against *Toxoplasma gondii* for chickens

Thabile Madlala [a], Victoria T. Adeleke [b], Moses Okpeku [a], Selaelo I. Tshilwane [c], Adebayo A. Adeniyi [d,e], Matthew A. Adeleke [a,*]

[a] Discipline of Genetics, School of Life Sciences, University of KwaZulu-Natal, Westville, P/Bag X54001, Durban 4000, South Africa
[b] Department of Chemical Engineering, Mangosuthu University of Technology, Durban 4031, South Africa
[c] Department of Veterinary Tropical Diseases, Faculty of Veterinary Science, University of Pretoria, Onderstepoort 0110, South Africa
[d] Department of Industrial Chemistry, Federal University, Oye-Ekiti, P.O Box 370111, Nigeria
[e] Department of Chemistry, Faculty of Natural and Agricultural Sciences, University of the Free State, Bloemfontein, South Africa

ARTICLE INFO

Keywords:
Toxoplasma gondii
Immunoinformatics
AMA1
Rhoptry
GRA7
Vaccine

ABSTRACT

Toxoplasmosis is a zoonotic disease caused by the protozoan parasite, *Toxoplasma gondii* known to infect almost all animals, including birds and humans globally. This disease has impacted the livestock industry and public health, where infection of domestic animals increases the zoonotic risk of transmission of infection to humans, threatening public health. Hence the need to discover novel and safe vaccines to fight against toxoplasmosis. In the current study, a novel multiepitope vaccine was designed using immunoinformatics techniques targeting *T. gondii* AMA1, GRA7 and ROP16 antigens, consisting of antigenic, immunogenic, non-allergenic and cytokine inducing T-cell (9 $CD8^+$ and 15 $CD4^+$) epitopes and four (4) B-cell epitopes fused together using AAY, KK and GPGPG linkers. The tertiary model of the proposed vaccine was predicted and validated to confirm the structural quality of the vaccine. The designed vaccine was highly antigenic (antigenicity = 0.6645), immunogenic (score = 2.89998), with molecular weight of 73.35 kDa, instability and aliphatic index of 28.70 and 64.10, respectively; and GRAVY of −0.363. The binding interaction, stability and flexibility were assessed with molecular docking and dynamics simulation, which revealed the proposed vaccine to have good structural interaction (binding affinity = −106.882 kcal/mol) and stability when docked with Toll like receptor-4 (TLR4). The results revealed that the Profilin-adjuvanted vaccine is promising, as it predicted induction of enhanced immune responses through the production of cytokines and antibodies critical in blocking host invasion.

Introduction

Toxoplasma gondii (T. gondii) is a protozoan parasite known to infect almost all warm-blooded animals and a causative agent of toxoplasmosis [1,2]. This parasite comprises a genome of ~ 80 Mb in size and 11 chromosomes [3,4]. *T. gondii* is an obligate intracellular parasite belonging to the Apicomplexan family, which harbours a great portion of infectious disease-causing parasites that are of medical and veterinary significance, such as causative agents of coccidiosis (*Eimeria spp.*), malaria (*Plasmodium falciparum*) and babesiosis (*Babesia spp.*) [5–7]. These parasites survive within the host through cycle series of parasite invasion, replication, and damage to host cells that greatly impact animal health and welfare.

Chicken meat is the main primary source of protein for human consumption globally, and the presence of *T. gondii* infection in chickens would indicate contamination of the environment and an increasing zoonotic risk for humans since chicken meat is a source of infection for humans when cooked poorly [8]. Studies indicate that the majority of human *T. gondii* infections (approximately 50%) are foodborne and result from consumption of contaminated meat [9,10]. This encourages the search for alternative strategies, such as antiparasitic drugs and developing vaccines to treat and prevent the spread of toxoplasmosis, which is of public health importance. With increasing studies focusing on prevalence and characterisation of *T. gondii* in chickens globally to

* Corresponding author.
E-mail address: adelekem@ukzn.ac.za (M.A. Adeleke).

https://doi.org/10.1016/j.jvacx.2023.100347
Received 23 July 2022; Received in revised form 23 June 2023; Accepted 6 July 2023
Available online 8 July 2023
2590-1362/© 2023 The Author(s). Published by Elsevier Ltd. This is an open access article under the CC BY-NC-ND license (http://creativecommons.org/licenses/by-nc-nd/4.0/).

confirm the importance of chicken as a source of toxoplasmasis for other warm-blooded animals [10–12], it is imperative to find alternative measures to mitigate the spread of the parasite from intermediate hosts. Developing vaccine against *T. gondii* in chickens is critical in hindering parasite infection transmission from chickens to other livestock or humans [13,14].

Vaccination approaches against *T. gondii* infection, including live attenuated, DNA, protein and multiepitope vaccines, have been previously evaluated in animal models (mice) to regulate and alleviate the parasite burden. The currently available prevention strategies against toxoplasmosis in domestic animals include Toxovax, the only approved live attenuated vaccine recommended to prevent *Toxoplasma* infection in sheep but its efficacy against chronic tissue cysts protection is still unknown [15]. Several drawbacks highlighted about Toxovax include short shelf life, possible parasite reversion to its virulent state and administration limitations [16]. This emphasises the basic criteria of an ideal vaccine that includes safety, stability, and cost-effectivity, with the ability to exert protection against infections or diseases by initiating immune responses. Various research has focused on different antigens found in the parasite to develop a peptide-based vaccine against *T. gondii*, namely, dense granule proteins, microneme proteins, rhoptry proteins and surface antigens and apical membrane antigens [17–20]. Research works focusing on *T. gondii* antigens as alternative control strategies through vaccination have been previously implemented, verifying the importance of improved control measures to alleviate toxoplasmosis [17,21–24].

Apical membrane antigen 1 (AMA1) is a crucial, highly conserved and immunogenic type 1 protein, expressed during the early stages of the *T. gondii* life cycle and secreted in the tachyzoite by the micronemes to facilitate attachment of the parasite to host cells [25]. With cooperation with other antigens, AMA1 facilitates the movement of *T. gondii* during initial host invasion by connecting the parasite and host cell membrane using rhoptry neck proteins (RONs) such as RON2, anchoring the parasite for invasion [7]. AMA1 as a candidate for DNA vaccine has been shown to stimulate strong cellular and humoral responses [25–28].

The dense granule protein (GRA) has been reported as the main component of *T. gondii* vacuoles, protecting tachyzoites, bradyzoites and the cyst wall [29]. These proteins play a serious role in the survival and the nutrient/waste exchange mechanism between host cells and parasites [30]. Some investigations involving the use of *T. gondii* antigens like dense granules (GRA) as vaccine candidates have shown great potential of inducing partial protection against *T. gondii* strains vaccine, with some drawbacks revealed as unstable, with the lowest degree of antigenicity [17,31,32].

The complexity of *Toxoplasma*'s life cycle resulting in tachyzoites, bradyzoites, and sporozoites currently drives the search for parasite stage-specific antigens with the potential of protecting infected hosts through the discovery of multiepitope-based vaccines, which is an attractive alternative for the prevention of toxoplasmosis [18]. Hence, the present study aimed to identify antigenic T-cell and B-cell epitopes through immunoinformatics techniques and design a potentially cost-efficient peptide-based vaccine by exploring the *T. gondii* antigens of warm-blooded animals, which serves as a base for experimental studies.

Methods and materials

Protein sequences availability and conserved sequences identification

The amino acid sequences of *T. gondii* apical membrane antigen-1 (AMA1), rhoptry protein-8, 16, and 18 (ROP8,16 and 18), and dense granule protein-7 (GRA7) isolated from the chicken host were identified and recovered from the National Centre for Biotechnology Information-NCBI (https://www.ncbi.nlm.nih.gov/protein/). The sequences were obtained in FASTA format and aligned through multiple sequence alignment (MSA) to generate conserved [33] sequences with a minimum of 15 amino acid residues. The MSA was performed using default parameters from the CLUSTALW online server (https://www.genome.jp/tools-bin/clustalw/) [34–37].

Antigenicity and transmembrane structural analysis

The identified conserved sequences were exposed to antigenicity testing using VaxiJen v2.0 Server (http://www.ddg-pharmfac.net/vaxijen/VaxiJen/VaxiJen.html), where selection criteria were set to a threshold of 0.4 and the target organism was a parasite. The sequences with a threshold =>0.4 were selected and identified as probable antigens. These antigens were further assessed for transmembrane helix properties using TMHMM v2.0 server (http://www.cbs.dtu.dk/services/TMHMM/).

Determination of T-cell binding epitopes

The conserved protein sequences that passed the transmembrane selection criteria were subjected to the NetCTL v1.2 tool (https://services.healthtech.dtu.dk/service.php?NetCTL-1.2), which is a server utilised to predict cytotoxic T lymphocytes (CTL) epitopes by generating potential nonamers using neural networks. The nonamers were identified using the server's default parameters, including epitope identification threshold of 0.75 and A1 supertype. The identified nonamers were used to predict $CD8^+$ epitopes from the IEDB online resources (http://tools.iedb.org/mhci). The prediction of $CD8^+$ epitopes was achieved using the Stabilized Matrix Base Method (SMM) and parameters including amino acid length of 9.0 residues, and IC_{50} values of epitopes < 250 [33]. The helper T-cell (HTL/$CD4^+$) epitopes were identified using the SMM-align (stabilisation matrix alignment) prediction method, allele length of 15 residues, and IC_{50} value < 250 from the IEDB online server (http://tools.iedb.org/mhcii/). Due to limited data focusing on chicken MHC alleles in the currently available immunoinformatic tools used for MHC -epitope predictions, human HLA alleles were chosen and used as an alternative for both epitope predictions. It has been reported that BF haplotypes of chicken consist of anchor residues similar to anchor residues found in mammalian MHC, supporting consideration and use of MHC B locus and human alleles for epitope predictions in this study [38,39].

The predicted T-cell epitopes were evaluated for antigenicity under a threshold of 0.5, to identify T-cell epitopes that were probable antigens. The identified $CD8^+$ T-cell epitopes were further tested for immunogenicity and conservancy using the IEDB online resources (http://tools.iedb.org/immunogenicity/, http://tools.iedb.org/conservancy/) [40,41] and allergenicity using AllerTop v2.0 tool to filter out allergenic sequences [42]. The identified HTL epitopes were further subjected to the IFNepitope and IL4pred servers (http://crdd.osdd.net/raghava/ifnepitope/, http://crdd.osdd.net/raghava/il4pred/) to predict epitopes that could induce cytokine interferon-gamma (IFN-γ) and interleukin-4 (IL-4).

Prediction of B-cell epitopes

The prediction of B-cell epitopes was achieved using the ABCpred online service (https://webs.iiitd.edu.in/raghava/abcpred/ABC_submission.html/), which employs an artificial neural network to identify B-cell regions in a protein sequence. The default parameters of the server were used in the prediction. The resulting shortlisted epitopes were inspected using similar immunoinformatics tools as the T-cell epitopes to determine their antigenicity, conservancy, and allergenicity.

Design of multiepitope vaccine

The final T- and B-cell epitopes identified from all the three antigens during the prediction stage and were regarded as potential vaccine candidates were joined together using AAY linkers for $CD8^+$ epitopes, GPGPG linkers for $CD4^+$ epitope, and KK linkers for the B-cell epitope. The Profilin adjuvant (accession number: KYF40283.1) was also

attached to the N-terminal of the vaccine with an EAAK linker. The addition of *T. gondii* profilin to the vaccine serves a crucial role since profilin is a protein known to function as a critical ligand recognised by receptors such as TLR11 and TLR2, crucial for activating host immune response via Th1 adaptive response during a parasite-host invasion [2]. Adding these linkers and an adjuvant to the vaccine construct aided in the flexibility and improved stability of the tertiary structure or model of the proposed vaccine, while the adjuvant enhanced the immunogenicity of the designed vaccine [22].

Assessment of antigenicity, allergenicity, solubility, and physicochemical properties of vaccine construct

The designed multiepitope vaccine construct sequence was exposed to Vaxijen v2.0, AllergenFP 1.0 server (https://ddg-pharm fac.net/AllergenFP/), and AllerTop v2.0 servers to predict the antigenicity and allergenicity of the construct [43]. These allergenicity classifier servers are based on E-descriptors and auto-cross covariance (ACC) transformations. Determining the allergenicity of the vaccine provides insight into the potential capability of the designed vaccine to induce an allergic reaction. The solubility of the vaccine construct was further evaluated by the SolPro server (https://scratch.proteomics.ics.uci.edu), which is an SVM-based tool used to accurately (~74% accuracy) predict the solubility of protein sequence through tenfold cross-validation [42]. The physicochemical properties of the vaccine were assessed via the ProtParam53 web server (https://web.expasy.org/protparam/) of the Expert Protein Analysis System (EXPASY), where the server was able to calculate parameters such as the amino acid composition of the vaccine, molecular weight, theoretical isoelectric point (pI), estimated half-life, instability, and aliphatic index and hydropathicity (GRAVY) [44].

Prediction of tertiary (3D) model, refinement, and validation of vaccine construct

The designed multiepitope vaccine sequence was subjected to the RaptorX server (http://raptorx.uchicago.edu) to predict and generate the vaccine tertiary structure. The resulting 3D structures underwent molecular refinement, where they were input into the GalaxyRefine server (http://galaxy.seoklab.org/cgi-bin/submit.cgi?type=REFINE) [45,46]. Refinement of the tertiary structure resulted in five refined vaccine construct models from a series of structural perturbations and relaxations by molecular dynamic simulation[47]. The tertiary structures were further assessed in reference to residues located in the outlier and favoured regions of the Ramachandran plot, generated from the online server PROCHECK [48]. ProSA-web (https://prosa.services.came.sbg.ac.at/prosa.php) was also employed to evaluate the overall quality of the designed 3D structure by generating a Z-score for confirmation.

Molecular docking of multiepitope vaccine with toll-like receptor

The molecular docking of the designed multiepitope vaccine (MEV) and toll-like receptor (TLR4) was achieved using an online server (AttractPep: http://www.attract.ph.tum.de/services/ATTRACT/attract.html) [49] and attract package locally installed from the Centre of High-Performance Computing (CHPC) Lengau cluster. Before molecular docking, the active and passive residues that served as the binding site of the TLR4 and MEV were identified by calculating solvent accessibility using the Naccess 2.1.1 package (http://wolf.bms.umist.ac.uk/naccess/) as described by Adeleke *et al.* [50]. The obtained residues/binding sites were then submitted to ATTRACT software (http://www.attract.ph.tum.de/services/ATTRACT/peptide.html) to perform docking of TLR4 and MEV [49]. The results obtained from the online ATTRACT docking were further submitted to CHPC to complete the molecular docking, where 50 structures were generated and assessed for binding energies. The docked model with the lowest binding energy, regarded as the best, was visualised using VMD and Chimera v1.14 software [51,52].

Molecular dynamics simulation of the vaccine construct

The tertiary models of the designed vaccine construct and Toll-like receptor-4 (TLR4) complex were introduced to an AMBER 14 package [53] to assess the stability of the MEV unbound and when docked to TLR4 through the molecular dynamics (MD) simulation technique. Both structures introduced to the AMBER 14 package underwent energy minimisation, where the input proteins were described using FF14SB [54]. The topologies of the vaccine structure and the addition of the missing ions (Cl^-) and hydrogen atoms to the orthorhombic solvation box filled with water molecules to neutralise the system were generated using the LEAP module of AMBER 14 [55]. The energy minimisation step was performed with 10,000 steps (steepest descents reached at 500 steps and 9500 conjugate gradients) followed by full minimisation at 2000 steps. The final MD simulation was run for 60 ns of NVT (constant number N, volume V and temperature T). Post MD analysis, parameters Root Mean Square Deviation (RMSD), Root Mean Square Fluctuations (RMSF), principal component analysis (PCA) plot, and dynamical cross-relational matrix (DCCM) analysis were performed, and the obtained results were documented graphically.

In silico codon optimisation, cloning, and expression of vaccine construct

Codon optimisation of the designed vaccine was performed using an online server, Java Codon Adaptation Tool (JCat: http://www.jcat.de/), where the MEV sequence was subjected to the server to estimate the codon adaptation index (CAI) and percentage GC content of the construct and an improved sequence of the construct with optimal expression probability when introduced to expression vector [56,57]. To analyse the JCat results, the SnapGene tool (https://www.snapgene.com/) was used to clone and express the optimised nucleotide vaccine sequence in the *E. coli* (strain K12) host. The restriction sites- HindIII (AAGCTT) and BamHI (GGATCC) were introduced to the final vaccine construct's C- and N-terminal sites and inserted into a suitable expression vector to assess the expression.

Vaccine construct in silico/online immune simulations

To evaluate the proposed vaccine's ability to induce immune response through the production of antibodies and immune cells, the vaccine peptide was subjected to an online C-ImmSim server (http://kraken.iac.rm.cnr.it/C-IMMSIM/). All simulation parameters were set at default, with a single injection and vaccine with no lipopolysaccharide (LPS) selected [58].

Results

Protein sequences availability and conserved sequences identification

A total of 52 amino acid sequences belonging to *T. gondii* antigens [AMA1, ROP(8, 16, and 18), and GRA7] obtained from the NCBI generated 56 conserved sequences when subjected to multiple sequence alignment (see Tables S1a,b, and c).

Antigenicity and transmembrane structural analysis

The generated conserved sequences were assessed for antigenicity using the set parameters of the server: threshold value set at ≥ 0.4 and target organism model set as a parasite, where out of the 52 conserved sequences, a total of 16 sequences for AMA1, 26 sequences for ROP(8,16 and 18) and seven (7) sequences for GRA7 were found to be antigenic and exhibited Vaxijen scores ranging from 0.4203 (Table S1b) to 1.7022

Table 1
$CD8^+$ T-cell predicted epitope candidates that overlapped with $CD4^+$ T-cell epitopes and interacted with different MHC I alleles.

Epitope(s)	HLA allele(s)	IC_{50}	Antigenicity	Allergenicity
AMA1				
AWKNLYFRA	HLA-A*30:01	183.218	1.7110	Non-allergen
LVWGSAYAR	HLA-A*31:01	37.71	0.6240	Non-allergen
	HLA-A*68:01	78.43		
	HLA-A*33:01	199.09		
NQALRGYRF	HLA-B*15:01	229.09	1.4794	Non-allergen
PNQALRGYR	HLA-A*31:01	143.04	0.9177	Non-allergen
ROP16				
LGSGHFGAV	HLA-A*02:06	30.307	0.9501	Non-allergen
MMIDVHGFG	HLA-A*02:03	45.493	1.2442	Non-allergen
	HLA-A*02:06	240.740		
NMMIDVHGF	HLA-B*15:01	114.815	1.1101	Non-allergen
	HLA-A*02:06	201.627		
	HLA-A*02:03	218.750		
SGHFGAVIK	HLA-A*30:01	99.763	1.2088	Non-allergen
GRA7				
EVHFRKRGV	HLA-A*68:02	57.89	1.4716	Non-allergen
FATAATASD	HLA-B*35:01	70.08	0.6417	Non-allergen
RKRGVRSDA	HLA-A*30:01	36.14	2.0735	Non-allergen

(Table S1a). These sequences were then used as input in the analysis of transmembrane properties, where a total of nine (9) conserved sequences for AMA1, five (5) sequences for ROP(8, 16, and 18), and three (3) sequences for GRA7 were detected to fulfil the criteria of the exomembrane properties (Tables S1a,b, and c). The exomembrane sequences were selected to predict $CD8^+$ and $CD4^+$ T-cell epitopes.

Determination of T-cell binding epitopes

The identified conserved sequences that passed transmembrane analysis were subjected to the NetCTL server to determine nonamers to induce $CD8^+$ T-cell epitopes. This server generated nonamers from the genomic sequences, which were further subjected to the IEDB server to predict T-cell epitopes. The selection criteria for predicting $CD8^+$ and $CD4^+$ T-cell epitope included the IC_{50} value < 250 and an amino acid length of 9 and 15, respectively. To determine AMA1 epitopes, a total of

Table 3
B-cell candidates were antigenic, 100% conserved and non-allergens.

Epitope	Antigenicity	ABCpred score	Allergenicity
AMA1			
PDAWQSACPNDAVKDA	0.6134	0.91	Non-allergen
PSDNPTQYVGDEGRGW	0.8395	0.83	Non-allergen
ROP16			
NNMMIDVHGFGHMLDM	0.9112	0.68	Non-allergen
GRA7			
EPDEQEEVHFRKRGVG	0.9012	0.77	Non-allergen

Table 2
$CD4^+$ T-cell predicted epitope candidates that are antigenic, conserved and overlap with $CD8^+$ T-cell epitopes and interact with different MHC II HLA-alleles.

Epitope(s)	HLA allele(s)	IC_{50}	Antigenicity	IFN-γ	IL-4	Allergenicity
AMA1						
AFLSKCPNQALRGYR	HLA-DRB1*01:01	115.00	1.0338	Inducer	Inducer	Non-allergen
ARALVYGSAFVAEGN	HLA-DRB1*01:01	53.00	1.3220	Inducer	Inducer	Non-allergen
	HLA-DRB1*15:01	111.00				
DAWQSACPNDAVKDA	HLA-DRB1*04:04	202.00	0.6574	Inducer	Inducer	Non-allergen
DNPTQYVGDEGRGWD	HLA-DRB3*01:01	97.00	0.7679	Inducer	Inducer	Non-allergen
	HLA-DRB5*01:01					
FLSKCPNQALRGYRF	HLA-DRB1*01:01	144.00	1.1204	Inducer	Inducer	Non-allergen
GGAWKNLYFRAAERR	HLA-DRB5*01:01	183.00	0.6663	Inducer	Inducer	Non-allergen
	HLA-DRB1*11:01	217.00				
IGGAWKNLYFRAAER	HLA-DRB1*11:01	227.00	0.6828	Inducer	Inducer	Non-allergen
KSSARALVYGSAFVA	HLA-DRB1*01:01	48.00	0.9438	Inducer	Inducer	Non-allergen
	HLA-DRB1*15:01	103.00				
LVYGSAFVAEGNPDA	HLA-DRB1*01:01	128.00	1.3226	Inducer	Inducer	Non-allergen
	HLA-DRB1*04:04	188.00				
	HLA-DRB1*04:01	242.00				
SAFVAEGNPDAWQSA	HLA-DRB1*01:01	216.00	1.1061	Inducer	Inducer	Non-allergen
	HLA-DRB1*04:04	233.00				
SDNPTQYVGDEGRGW	HLA-DRB3*01:01	100.00	0.8846	Inducer	Inducer	Non-allergen
SIGGAWKNLYFRAAE	HLA-DRB1*11:01	231.00	0.5996	Inducer	Inducer	Non-allergen
ROP16						
ARAELVKTIRQELDV	HLA-DRB1*07:01	159.00	0.6346	Inducer	Inducer	Non-allergen
	HLA-DRB4*01:01	195.00				
	HLA-DRB1*11:01	206.00				
DVKLNNMMIDVHGFG	HLA-DRB4*01:01	246.00	1.1251	Inducer	Inducer	Non-allergen
LGSGHFGAVIKASLD	HLA-DRB1*09:01	94.00	0.8969	Inducer	Inducer	Non-allergen
	HLA-DRB1*01:01	106.00				
	HLA-DRB1*11:01	111.00				
	HLA-DRB1*04:05	145.00				
	HLA-DRB1*07:01	196.00				
LPLCQMTLTLPENKA	HLA-DRB1*01:01	240.00	0.5526	Inducer	Inducer	Non-allergen
RDKLVAKGLTLTETV	HLA-DRB1*01:01	109.00	0.6831	Inducer	Inducer	Non-allergen
GRA7						
DEQEEVHFRKRGVGS	HLA-DRB1*11:01	113.00	1.1438	Inducer	Inducer	Non-allergen
DEQEEVHFRKRGVRS	HLA-DRB1*11:01	113.00	1.2338	Inducer	Inducer	Non-allergen
EQEEVHFRKRGVGSD	HLA-DRB1*11:01	115.00	1.2501	Inducer	Inducer	Non-allergen
PQFATAATASDDELM	HLA-DRB1*11:01	115.00	0.6795	Inducer	Inducer	Non-allergen
QEEVHFRKRGVRSDA	HLA-DRB1*11:01	115.00	1.6122	Inducer	Inducer	Non-allergen

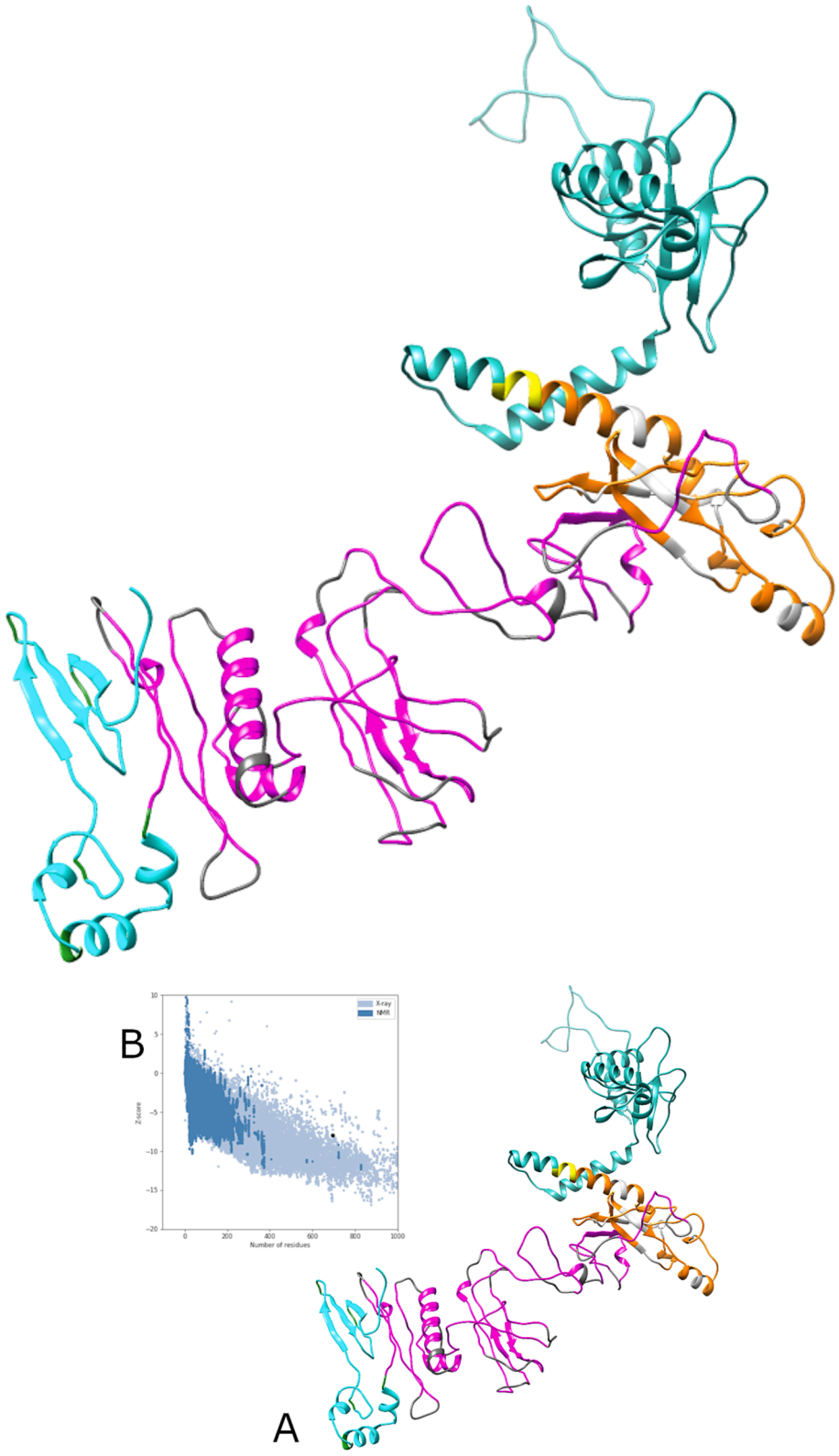

Fig. 1. Structural prediction and validation of proposed multiepitope vaccine showing (A) Final predicted tertiary model of designed vaccine. The adjuvant is noted as sea green, $CD8^+$ epitopes (orange), $CD4^+$ epitopes (Magenta), B-cells (Cyan) and linkers highlighted as: EAAAK (yellow), AAY (light gray), GPGPG (dim gray) and KK (green) and (B) Structural validation analysis of designed vaccine with ProSA-web validation server of 3D structure showing Z-score(−7.94). (For interpretation of the references to colour in this figure legend, the reader is referred to the web version of this article.)

453 nonamers were detected as sequences with the potential to bind to the major histocompatibility complex (MHC) molecules class I. These nonamers were further subjected to the MHC-I IEDB prediction tool, where 88 $CD8^+$ T-cell epitopes were predicted. The identified epitopes were evaluated for antigenicity and immunogenicity, where a total of 56 epitopes were found to be antigenic. The immunogenicity analysis further reduced the number of identified sequences to only 27 $CD8^+$ T-cell epitopes that were antigenic and immunogenic. More scrutinising analyses, such as conservancy and allergenicity were performed from the identified antigenic and immunogenic epitopes, resulting in the identification of the final four (4) conserved and non-allergenic $CD8^+$ T-cell epitopes. The detailed summary of the final predicted $CD8^+$ T-cell epitopes, showing the IC_{50}, antigenicity, immunogenicity, and allergenicity scores, are presented in Table 1. The procedure for AMA1 was repeated for ROP(8,16 and 18) and GRA7 epitopes detailed in Table S2.

The prediction of $CD4^+$ T-cell epitopes resulted in the identification of 146 peptides (AMA1) from the IEDB prediction tool. These peptides represented potential $CD4^+$ T-cell epitopes that could bind to MHC class II molecules. When testing for antigenicity, the number of identified peptides reduced drastically to 96 antigenic epitopes. Following this, the predicted antigenic $CD4^+$ T-cell epitopes were assessed for their ability to induce IFN-γ and IL-4. For each analysis, 28 and 22 epitopes were identified as inducers, respectively. Only 12 $CD4^+$ Tcell epitopes passed the conservancy and allergenicity analysis from the identified peptides and were regarded as the final potential vaccine candidates (Table 2). Similar prediction procedure was employed for ROP(8,16 and 18) and GRA7 epitopes as shown in Table S2.

Prediction of B-cell epitopes

The prediction of B-cell epitopes was achieved using the ABCpred server, where a total of 61 AMA1 epitopes were detected by employing the recurrent neural network at a default threshold of 0.51. The identified epitopes were further subjected to Vaxijen and AllerTop servers to evaluate their antigenicity and allergenicity, where a total of 42 B-cell epitopes were identified as antigenic. From the identified 42 sequences, 20 epitopes were found to be non-allergen. The non-allergenic epitopes were further assessed for conservancy, where the analysis revealed only two (2) B-cell epitopes to be conserved, hence regarded as the final selected B-cell epitopes (Table 3). The prediction of these epitopes was crucial for the multiepitope vaccine design, as this suggested possible activation of the specific humoral response.

The procedure used to predict AMA1 B-cells was also employed to determine ROP(8,16 and 18) and GRA7 epitopes using the antigens' conserved sequences. The overall results obtained for both antigens were summarised and presented in Table S2, with the summary of the final predicted T- and B-cell epitopes shown in Tables 1, 2 and 3. Post-prediction analysis of the rhoptry antigens showed that all the final identified T-cell epitopes belonged to ROP16. From the identified final respective $CD8^+$ and $CD4^+$ T-cell epitopes, the most antigenic sequences were observed as RKRGVRSDA (VaxiJen score = 2.0735) and QEEVHFRKRGVRSDA (Vaxijen score = 1.6122) from the GRA7 antigen, whereas the sequence with the lowest antigenicity was noted from sequences obtained from AMA1 (LVWGSAYAR; VaxiJen score = 0.6241) and ROP16 (LPLCQMTLTLPENKA; VaxiJen score = 0.5526).

Design of multiepitope vaccine

The final obtained antigenic, conserved, and non-allergenic T and B-cell epitopes from the three antigens were fused using flexible linkers. Keeping in mind the size of the vaccine construct, only the top three (3) $CD8^+$ and five (5) $CD4^+$ T-cell epitopes and all the B-cell epitopes identified to be highly antigenic (highest VaxiJen score) were selected from each antigen and joined together to form the predicted vaccine construct. This resulted in a final predicted vaccine construct consisting of three (3) AMA1 + three (3) ROP16 + three (3) GRA7 CTL/$CD8^+$ epitopes and five (5) AMA1 + five (5) ROP16 + five (5) GRA7 HTL/$CD4^+$ epitopes respectively and four (4) B-cell epitopes joined using AAY, GPGPG linkers and KK linkers, respectively. The Profilin adjuvant (accession number: KYF40283.1) was attached to the N-terminal of the vaccine construct with the aid of the EAAAK linker. The attachment of an adjuvant to the designed vaccine construct enhanced the immunogenicity of the construct and composition of the vaccine, resulting in a multiepitope with 695 amino acid residues.

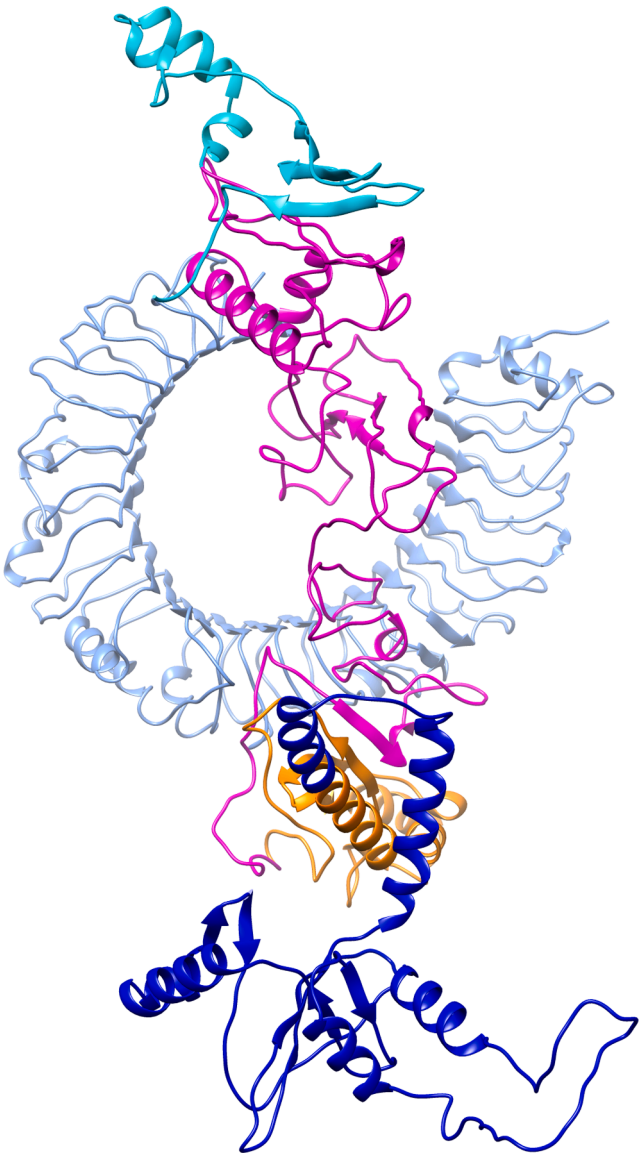

Fig. 2. The refined tertiary model of MEV construct docked to toll-like receptor-4 (TLR4) complex; where TLR4 is observed as cornflower blue and MEV is divide into CD8 (Orange), CD4 (Magenta), B-cells (Cyan) and adjuvant (Blue). (For interpretation of the references to colour in this figure legend, the reader is referred to the web version of this article.)

Assessment of antigenicity, allergenicity, solubility, and physicochemical properties of vaccine construct

To validate the efficiency of the designed multiepitope vaccine, the construct's sequence was subjected to antigenicity, immunogenicity, allergenicity, and physiochemical properties assessment. These assessments revealed the designed vaccine to be non-allergenic, antigenic with a Vaxijen score of 0.6645 and immunogenic (score = 2.89998). When evaluating solubility for the final vaccine using Solpro, the obtained

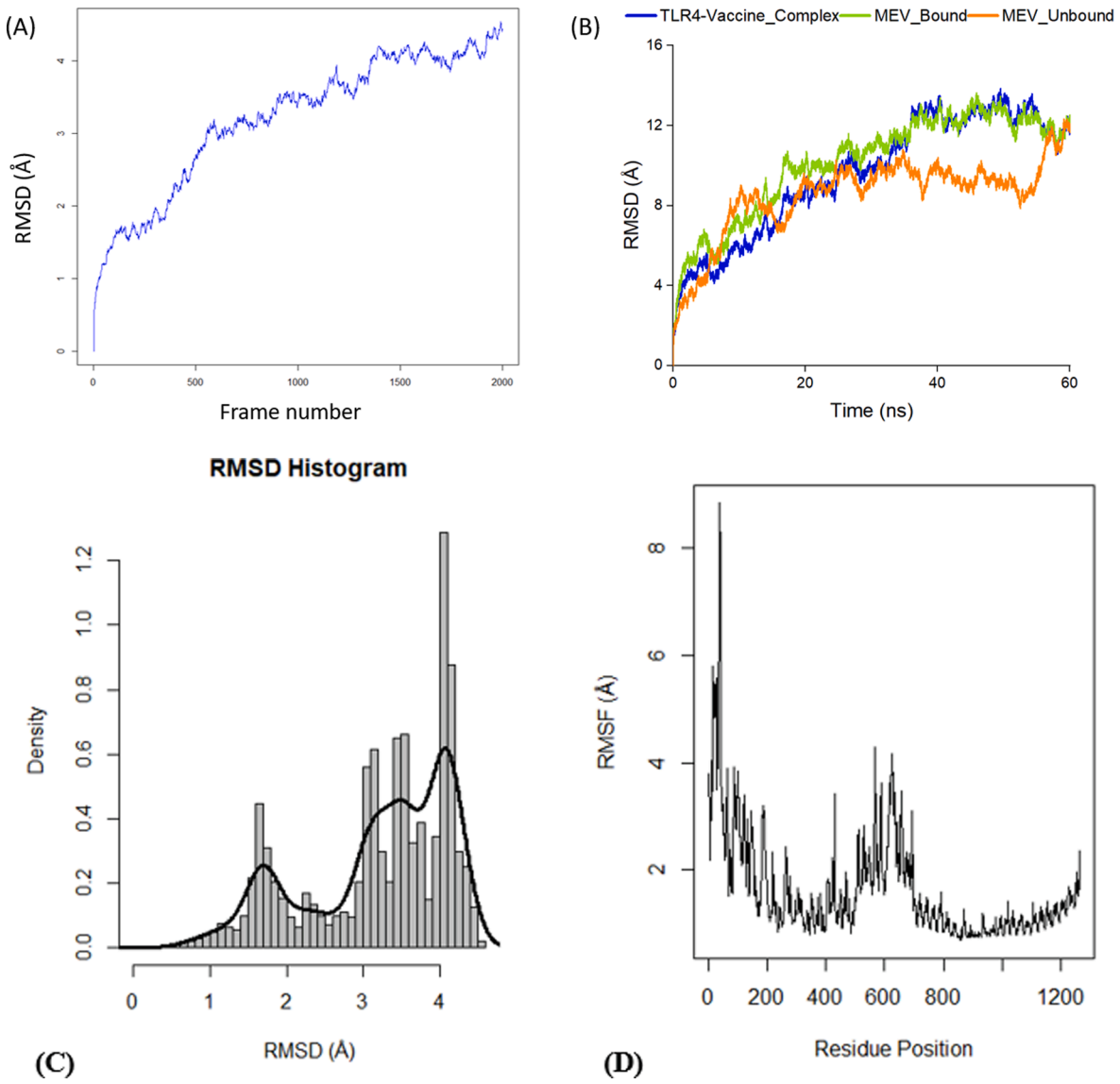

Fig. 3. Molecular dynamics outputs showing (A) RMSD plot of the complex after MDS generated for 2000 frames, (B) RMDS plot comparing MEV before and after MDS, (C) RMSD histogram and (D) RMSF plot of MEV-TLR4 complex.

solubility probability of 0.7086 identified our vaccine as highly soluble. The physiochemical properties evaluated via the ProtParam server showed that the designed vaccine had a molecular weight of 73.35 kDa, the theoretical pI of 8.29, indicating the vaccine's basic nature, with the instability and aliphatic index of 28.70 and 64.10, respectively. The estimated half-life obtained when performing the *in vivo* analyses in yeast and *E. coli* was recorded to be over 20 h (hrs) and greater than 10 h in *E. coli*. The assessment of the grand average of hydropathicity (GRAVY) of the vaccine protein provided insight into the protein solubility, where positive GRAVY is regarded as hydrophobic and negative GRAVY as hydrophilic. In this study, the GRAVY obtained for the designed vaccine protein was −0.363, indicating the hydrophilic nature of the vaccine that can easily interact with water molecules [50].

Prediction of tertiary (3D) model, refinement, and validation of vaccine construct

The tertiary structure prediction and modelling of the MEV construct was done using the RaptorX online server tool, which generated five potential models subjected for validation in the ProSA server to assess the quality of the designed models. Model 2 was selected as the best model, with a Z score of −7.69. The best predicted model was also selected based on the following criteria: GDT-HA (0.9514), RMSD (0.414), Molprobity (2.044), Clash score (12.4), Poor rotamers (0.4), and Ramachandran plot (93.2). This model was further subjected to the Refinement GalaxyRefine tool to improve and modify the vaccine structure by adding missing residues. The server also predicted five potentially refined models, where the best refined model exhibiting higher GDT-HA, low RMSD, low Molprobity, higher % reduction clash score, low poor rotamers, and higher Rama favoured was selected. The best model selected from the refined structures was Model 1 (Fig. 1A),

Table 4
The energy composition (kcal/mol) of the MEV-TLR4 complex from MMGBSA.

Energy Component	Average	Std. error of mean	Std. deviation
Van der Waal Energy	−138.8667	0.4135	15.4512
Electrostatic	−649.2601	2.4655	92.1182
Solvation of free energy	753.2494	2.5198	94.1493
Non-polar solvation energy	−19.8993	0.0601	2.2463
Gas phase energy	−788.1267	2.5387	94.8537
Solvation free energy	733.3501	2.5077	93.6966
Binding energy	−54.7767	0.6426	

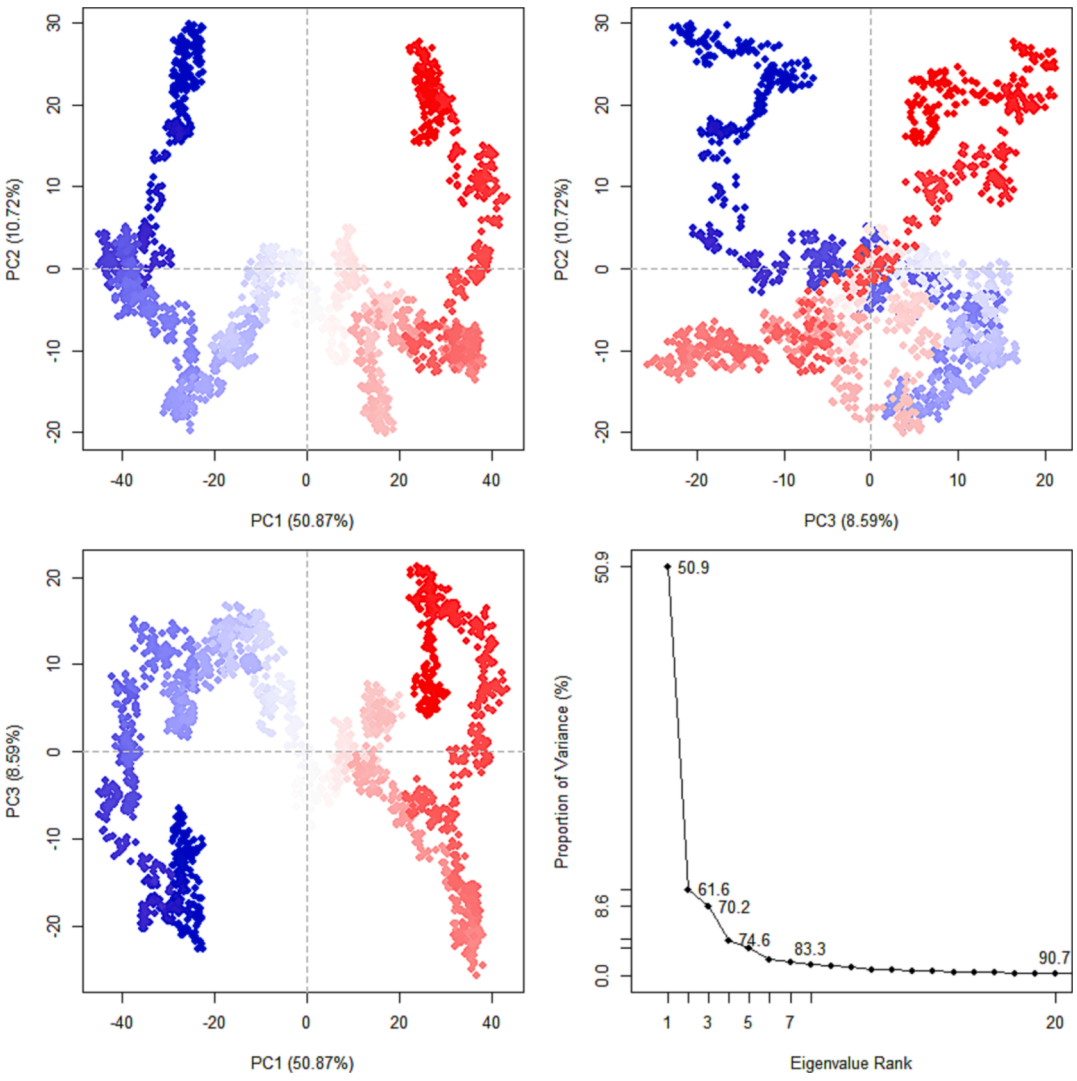

Fig. 4. (A) PCA analysis of MEV-TLR4 complex showing plots of PC1 vs PC2, PC1 vs PC3 and PC2 vs PC3, and (B) Dynamical cross-correlation map of vaccine construct.

which was further subjected to ProSA for validation. The server revealed the overall model quality of the refined model with a Z-score of −7.94 (Fig. 1B), which was observed to lie within the score range of the comparable-sized native proteins, indicating good overall model quality.

Molecular docking of multiepitope vaccine with toll-like receptor

The final refined 3D model of the designed vaccine construct was docked with TLR4 complex to evaluate their interaction, stability, and binding affinities/ energies using the pepAttract software and CHPC, Lengau cluster. The docking of these complexes resulted in 50 binding confirmations of docked complexes, where the observed binding affinities of the complexes ranged from −3.826 kcal/mol to −151.159 kcal/mol. The best docked complex selected was model 6, containing the lowest binding affinity of −106.882 kcal/mol (Fig. 2), suggesting proper binding and interaction between the vaccine model and receptor.

Molecular dynamics simulation (MDS) of the vaccine construct

The MDS was performed to evaluate the stability and binding interaction between the docked vaccine complex and TLR4 parameters, root mean square deviation (RMSD) and root mean square fluctuation (RMSF), as shown in Fig. 3A, B and C. To determine the stability and structural flexibility of the MEV complex, the RMSD and RMSF of the complex were compared and examined for 60 ns. The fluctuations for the MEV-TLR4 complex were relatively low, showing the stability and strong interaction between the designed vaccine and the TLR4 complex. The RMSD outputs revealed minor complex fluctuations after molecular dynamic simulation, which were observed ranging between 1 and 4 Å and reaching equilibrium after 4 Å (Fig. 3A). When comparing structural flexibility between MEV before and after MDS, it was noted the MEV unbound (before docking) exhibited more fluctuations in the system, whereas the MEV bound (after docking) showed more stability with complex, and MEV bound reaching equilibrium at 12 Å in 40 ns (Fig. 3B). This reflected a fairly stable interaction between our designed vaccine and TLR4, further confirmed by the RMSD histogram in Fig. 3C. The RMSF plot showed fluctuations of the side chain atoms of docked complex observed at 5–100 (highest peak at 8 Å), 400–500, and 600–700 residues (with a peak height of 4 Å) (Fig. 3D). The difference in peak height between fluctuations may suggest high flexibility and stability of amino acid residues in the vaccine throughout the simulation, further confirming the overall stability of the vaccine complex.

The binding energy of the vaccine-TLR complex and other energy

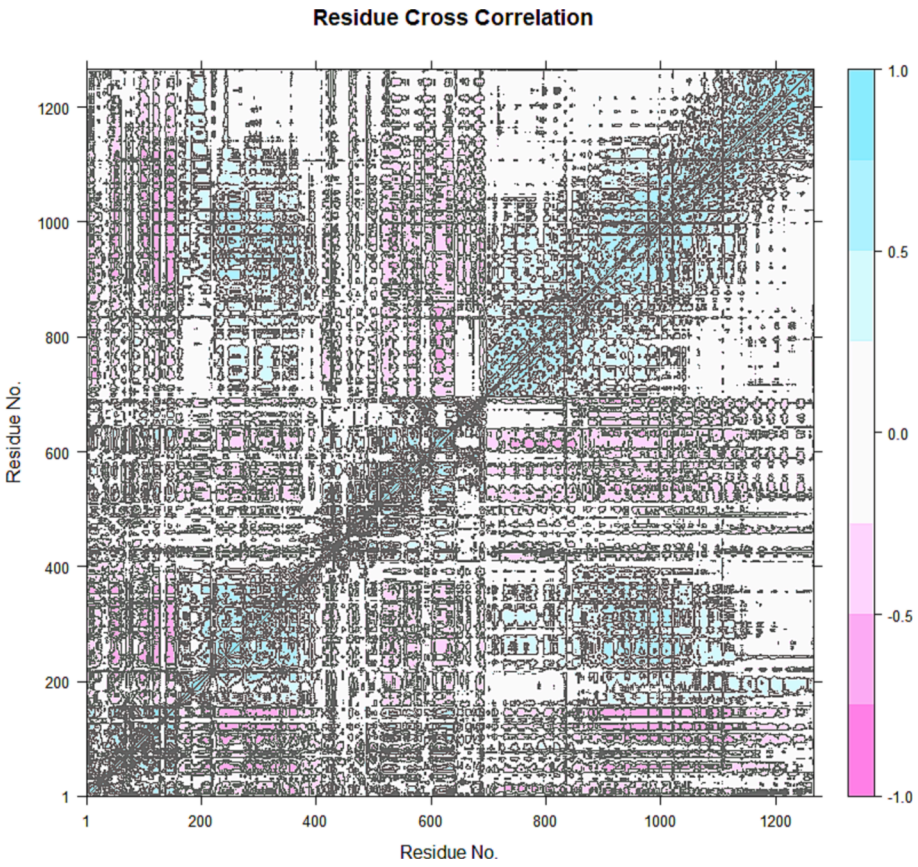

Fig. 4. (*continued*).

components were further assessed through the MMGBSA analysis, and the results are summarised in Table 4. The interaction of MEV and TLR4 receptor was also observed through the PCA analysis, where from the outputs it was noted that the clustering of residues in PC2 vs PC3 indicated a strong correlation of the MEV-TLR4 complex. This was noted by the uninterrupted clustering marked in blue, white, and red to show transitions between the residues (Fig. 4A). The DCCM map of the vaccine construct based on C-alpha atoms revealed high diagonal cross-correlation, where the blue colour represented a positive correlation and the pink represented negative correlation (Fig. 4B).

In silico codon optimisation, cloning and expression of vaccine construct

Codon optimisation of the designed vaccine was achieved by inputting the protein sequence of the proposed vaccine into the JCat server. The sequence was optimised for optimal expression in the *E. coli* expression system (strain K12 as a host). The improved codon sequence of the designed MEV was observed to have 2085 nucleotides, a CAI of 0.98, and an average GC percentage content of 54.96%. Since the ideal criteria for optimisation include GC content and a CAI value ranging from 30 to 70% and 0.8–1.0, the obtained results showed that the designed vaccine has a high probability of good expression in an *E. coli* host. The graphical illustration of the codon optimisation for our vaccine is represented in Fig. 5A. Prior to *in silico* cloning, the optimised MEV sequence was inspected for *HindIII* and *BamHI* restriction enzyme sites. Since they were not found in the vaccine sequence, these enzymes were further used for *in silico* cloning where the adapted codon sequence of the designed vaccine was inserted into the pET-28a (+) vector using SnapGene software resulting in a clone consisting of 7105 bp (Fig. 5B).

Vaccine construct in silico/ online immune simulation

The online immune simulation of the designed vaccine revealed different immune profiles consistent with the expected immune response of the host, where the vaccine was observed to induce primary immune response at initial administration of the antigens by stimulating an increased antibody level of IgM between day 0–5 post initial injection (Fig. 6A). This was followed by an increase in IgM + IgG, IgG1 + IgG2 and IgG1, indicating the induction of secondary and tertiary immune response of the host (Fig. 6A). The presence of memory $CD8^+$ T-cytotoxic lymphocytes-TC (Fig. 6B) and B memory cells (Fig. 6C) is crucial for the protection of the host as they retain the memory of the antigen to prevent any possibilities of host reinfection. The gradual increase of cytokines such as IFN-γ, TGF-b, IL-10, IL-23, and IL-12 (Fig. 6D) post-injection of vaccine antigens into the simulation further confirms and validates the inclusion of epitopes previously identified as IFN-γ and IL-4 inducers into the proposed vaccine. These findings greatly improve the designed vaccine's efficacy and capability in inducing host immune response (Fig. 6B), correlating with the prediction of IFN-γ epitopes in the vaccine.

Discussion

Toxoplasmosis currently poses a great threat to animals and humans worldwide, with ~ 30% of the world population suffering from this disease [22]. With limitations on the treatments currently available to effectively combat and eradicate this parasite, the need for novel alternative strategies to treat and prevent this disease, such as developing an efficient and safe novel vaccine by exploring the parasite invasion machinery (antigens) is crucial. To control *T. gondii* infections, DNA vaccination has been considered an appropriate strategy to fight against toxoplasmosis through the activation of long-term host immune

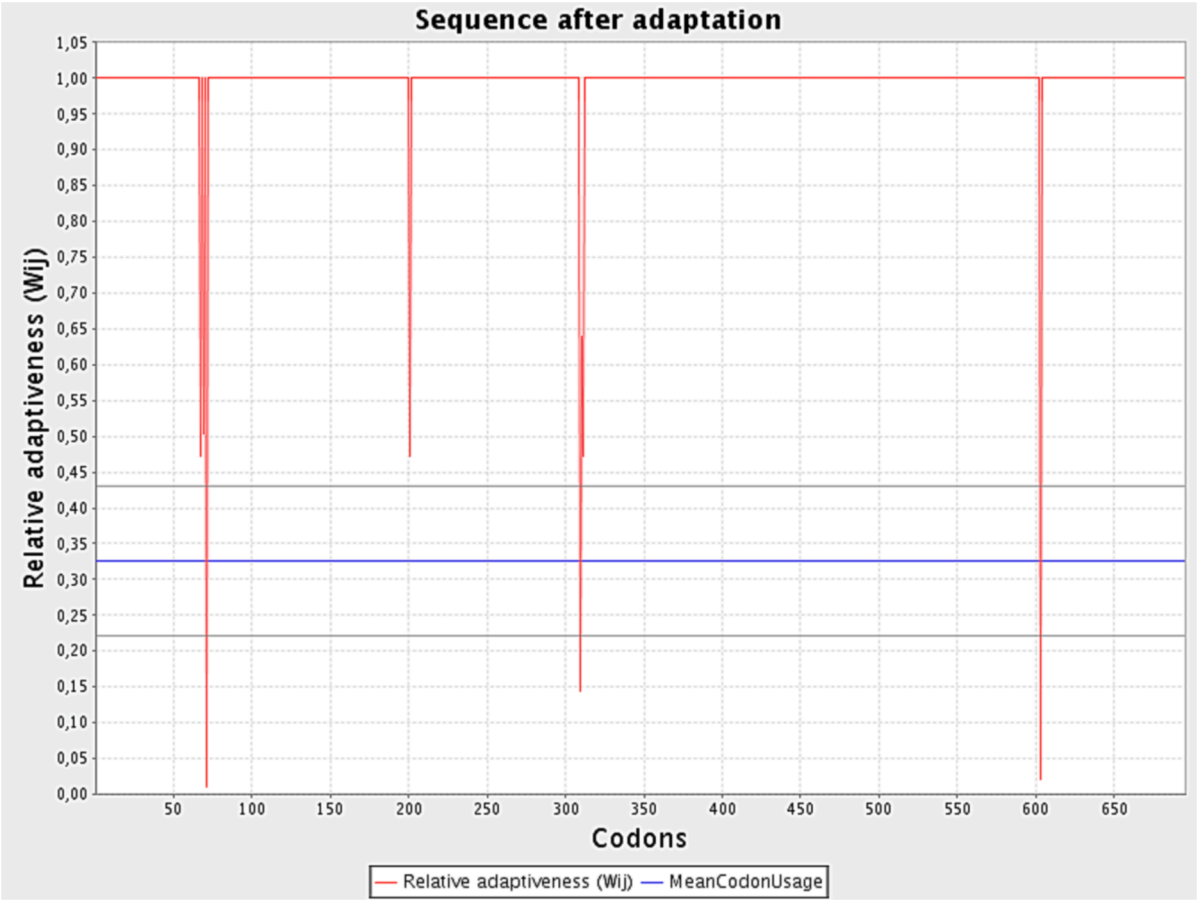

Fig. 5. *In silico* codon optimisation and cloning outputs showing (A) Graphical illustration of codon usage during optimisation of MEV sequence, where the red line represents the relative adaptiveness and the blue line represents mean codon usage. (B) *In silico* cloning of vaccine construct sequence into the pET28a(+) expression vector; the gene representing the vaccine sequence is highlighted in red, within a black vector. (For interpretation of the references to colour in this figure legend, the reader is referred to the web version of this article.)

responses [56].

The present study explored critical *T. gondii* proteins including AMA, ROP, and GRA proteins, that form part of the parasite's life cycle and invasion mechanism used for host invasion. The immunoinformatics techniques successfully predicted 20 AMA1, 10 ROP16, and 9 GRA7 epitopes that were conserved, antigenic, and highly immunogenic. The use of immunoinformatics techniques for epitope prediction proved advantageous, as they drastically reduced the time for the analysis procedures and showed high precision in epitope prediction [59]. Previous research has implemented these techniques in the search for control strategies against toxoplasmosis [17,21,22], verifying the importance and need for current and improved control measures to alleviate toxoplasmosis.

The predicted multiepitope DNA vaccine with a profilin adjuvant comprised 695 amino acid residues and molecular weight of 73.35 kDa. Considering drawbacks noted with multieiptopes vaccines such as low antigenicity and immunogenicity, construction of the proposed vaccine in this study selected the best B and T-cells based on their high antigenicicty score and the inclusion of adjuvant in DNA vaccine greatly improved the immunogenicity of the construct; allowing for an enhanced immune response with a lower dose of inactivated antigen [60–62]. This can be confirmed by immunogenicity scores of the designed vaccine obtained before (immunogenic score = 2.17697) and after (immunogenic score = 2.89998) the addition of adjuvant. The online immune simulation analysis profiles (Fig. S1A) also showed that less antigen dose (indicated by the black line) was needed to stimulate the response of the B-cell population when the profilin-adjuvanted MEV (500 at day 0–5 and 280 between day 15–20) was injected into the system compared to injection of MEV without the adjuvant (700 at day 0–5 and 480 between day 15–20). This difference can also be observed when comparing antibody levels in plasma B lymphocyte profiles in Fig. S1B.

The vaccine construct was assessed for physiochemical properties, where it was predicted to be basic and thermostable with theoretical pI of 8.29, instability and aliphatic index of 28.70 and 64.10. The observed GRAVY of −0.363 indicated the proposed vaccine as hydrophilic, implying easy interaction with water molecules. With the instability index and molecular weight < 40 and < 110 kDa, respectively, the designed vaccine fits the criteria of a stable vaccine candidate appropriate for development [22,56,63]. The structural validation revealed that the proposed refined vaccine model had a quality z-score of −7.94 (Fig. 1B), indicating that the overall structural quality of the designed vaccine model was satisfactory. When exposed to molecular docking with TLR4, the resulting vaccine complex (Fig. 2) exhibited strong hydrogen bonding interaction with the lowest binding affinity recorded as −151.159 kcal/mol. The interaction observed with the TLR and designed vaccine suggests that the proposed MEV can potentially activate TLRs in the presence of *T. gondii* infection, stimulating antigen-presenting cells (APCs); T- and B-cell activation resulting in an improved immune response against the parasite.

The binding interactions, stability, and flexibility of the docked MEV-TLR4 complex was further confirmed by molecular dynamics simulation

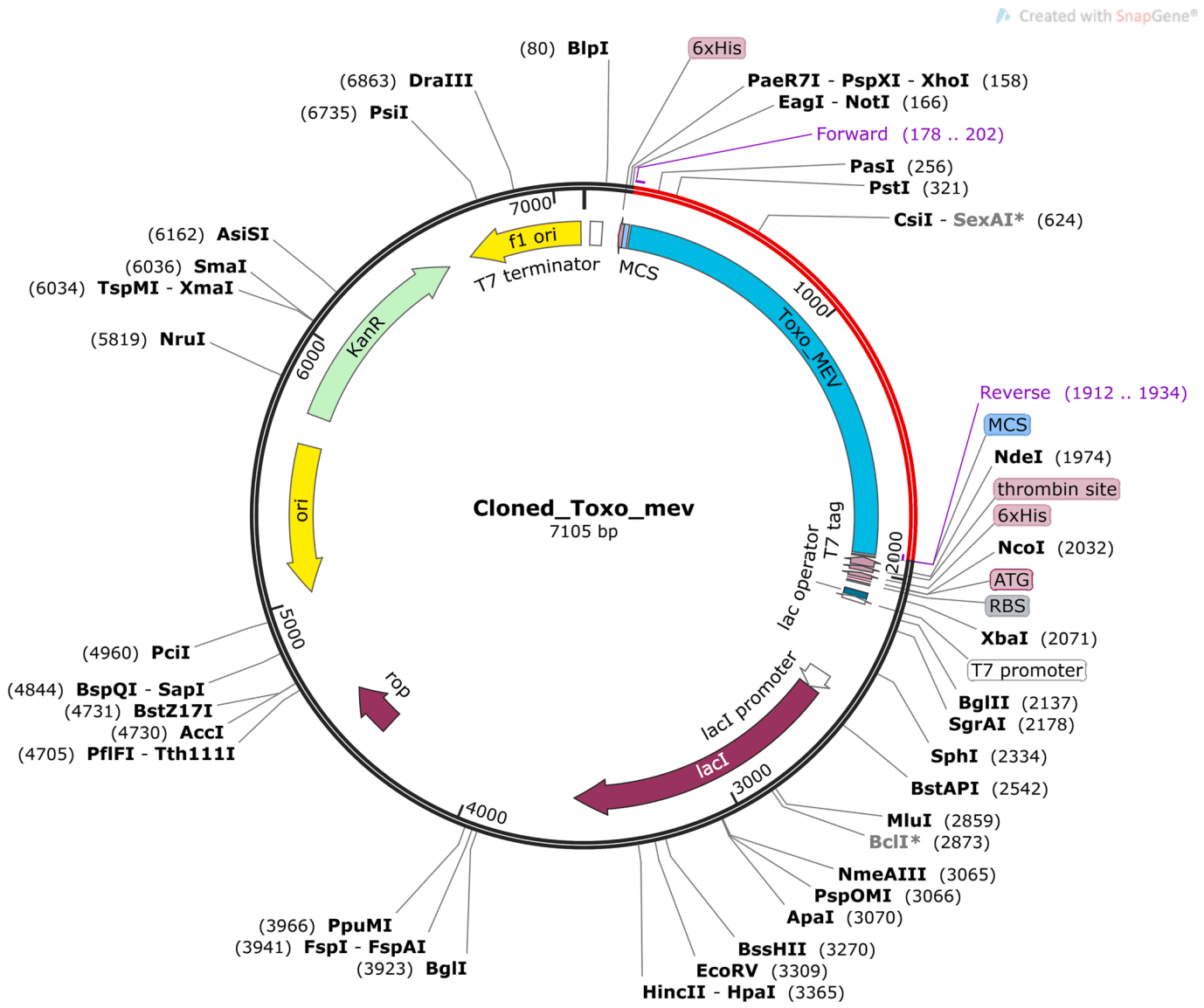

Fig. 5. (*continued*).

outputs MMBSA energy composition results (Table 4), RMSD and RMSF (Fig. 3). The results obtained post molecular dynamics simulation of the MEV-TLR4 complex further assured the stability of the proposed vaccine when potentially administered or injected into living hosts. This was further validated by the *in silico* codon optimisation and cloning findings, where the designed vaccine presented an optimal CAI value (0.98) and GC content (54.96), suggesting the successful cloning and expression of the vaccine in a suited expression vector (Fig. 5).

The *T. gondii* protective immunity is linked to innate responses where protection against infection is achieved through the production of dendritic cells and macrophages at the site of infection [64]. Production of these cells triggers the secretion of cytokines IFN- γ and IL-12, further stimulating the production of $CD8^+$ and $CD4^+$ T-cells [65]. The production of these T-lymphocytes during *Toxoplasma* infection exerts cytotoxic activity against tachyzoites and regulates immune response [66]. This supports the immune simulation findings in this study, where the initial dose of the designed MEV activated the presence of T cytotoxic (TC) and B memory cells (Fig. 6B&C), which is valuable for protecting the host against *T. gondii* infection. The initial dose of the proposed vaccine was observed to induce IgM antibodies, representing the primary immune response. This response was shortly followed by the production of antibodies involved in secondary (i.e., IgM + IgG) and tertiary response indicated by IgG1 + IgG2, IgG1, and IgG2 (Fig. 6A). The elevated levels of these antibodies, especially IgG1 and IgG2 after injection of the vaccine showed great advantage for the proposed vaccine as it was a good indicator of induction of Th1 immune response [63,67].The *in silico* immune simulation results revealed that antigen injection of our MEV induced increased production of IFN-γ and IL-2 (Fig. 6D), confirming the effectiveness of the designed vaccine.

The overall findings leading to the design of the proposed vaccine, especially immune simulation analyses, are imperative during the discovery and development of the novel vaccine, as they provide insight into real-life immune responses that the proposed vaccine could exert towards *T. gondii* infection. The prediction and development of our proposed vaccine proved advantageous in designing a highly stable vaccine specifically designed for augmented potency through exploration of flexibility of antigens and the combination of epitopes from different antigens. Using immunoinformatics techniques allowed for easy vaccine synthesis at high specificity by surpassing time-consuming wet lab experiments [68]. The physiochemical properties observed in this study further support any future production of the designed vaccine. Since the prediction and design of our MEV are computationally based, future studies focusing on laboratory-based validation of the proposed vaccine to evaluate its efficiency are needed.

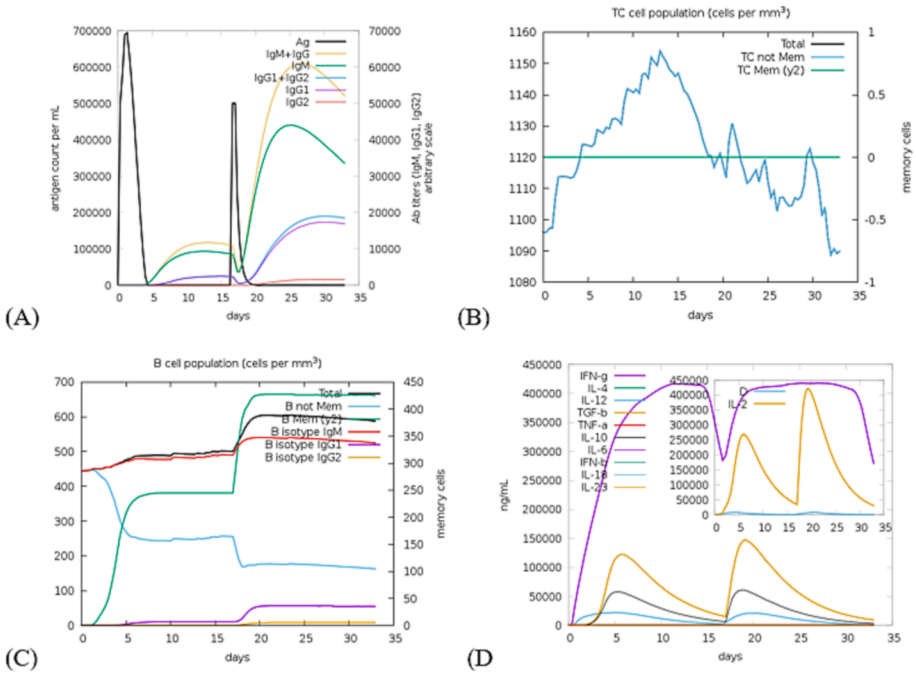

Fig. 6. Immune response outputs of the designed multiepitope vaccine (MEV) through an online immune simulation server, C-IMMSIM. a) Immunoglobulin production in response to antigen injection (black vertical line). b) Cytotoxic T cell memory cell for $CD8^{+}$. c) B-cell population after two antigen injections. d) Cytokines and interleukin production in response to antigen.

Conclusion

The severe impact *T. gondii* infections continue to inflict on warm-blooded animals and humans globally currently drives the urge to discover novel control measures to eliminate the parasite, including any traces of cyst tissues in meats. One such measure currently being explored in research includes discovering novel multiepitope-based vaccines. This approach has been noted as advantageous in vaccine development as it encourages the development of novel and effective vaccines in a short time and at a relatively low cost. The current study designed a promising multiepitope vaccine from a cocktail of *T. gondii* antigens, consisting of diverse T- cells (9 $CD8^{+}$ and 15 $CD4^{+}$) and 4 B-cell epitopes using immunoinformatics techniques. From the *in silico* experiments explored, the designed vaccine was highly antigenic, non-allergenic, and immunogenic. It showed great promise in potentially conferring complete host protection as it effectively elicited host immune response through induction and production of cytokines. These findings were achieved through an innovative approach and should be valuable for future studies focusing on vaccine development against *T. gondii*.

Ethical approval

Not applicable.

Funding Sources

This study is based on the research supported by the National Research Foundation (NRF) of South Africa (Grant number: 130692 and Thuthuka Grant number: 129840).

Declaration of Competing Interest

The authors declare the following financial interests/personal relationships which may be considered as potential competing interests: Matthew A. Adeleke reports financial support was provided by National Research Foundation (Grant number: 130692). Thabile Madlala reports financial support was provided by National Research Foundation (NRF) of South Africa (Thuthuka Grant number: 129840).

Data availability

Data will be made available on request.

Acknowledgements

The authors also wish to acknowledge the Centre for High-Performance Computing, South Africa, for the computer programs and facilities utilised in this project.

Appendix A. Supplementary material

Supplementary data to this article can be found online at https://doi.org/10.1016/j.jvacx.2023.100347.

References

[1] Ducournau C, Moiré N, Carpentier R, Cantin P, Herkt C, Lantier I, et al. Effective Nanoparticle-Based Nasal Vaccine Against Latent and Congenital Toxoplasmosis in Sheep. Front Immunol Sep. 2020;11. https://doi.org/10.3389/fimmu.2020.02183.
[2] Gao Qi, Zhang N-Z, Zhang F-K, Wang M, Hu L-Y, Zhu X-Q. Immune response and protective effect against chronic Toxoplasma gondii infection induced by vaccination with a DNA vaccine encoding profilin. BMC Infect Dis 2018;18(1).
[3] Kissinger JC, Gajria B, Li L, Paulsen IT, Roos DS. ToxoDB: Accessing the Toxoplasma gondii genome. Nucleic Acids Res vol. 31, no. 1. Oxford University Press, pp. 234–236, Jan. 01, 2003, doi: 10.1093/nar/gkg072.
[4] Lau YL, et al. Deciphering the draft genome of Toxoplasma gondii RH strain. PLoS One 2016; 11(6), Jun. 2016, doi: 10.1371/journal.pone.0157901.
[5] Liu T, Huang J, Li Y, Ehsan M, Wang S, Zhou Z, et al. Molecular characterisation and the protective immunity evaluation of Eimeria maxima surface antigen gene. Parasites Vectors 2018;11(1).
[6] Soutter F, Werling D, Tomley FM, Blake DP. Poultry Coccidiosis: Design and Interpretation of Vaccine Studies. Front Vet Sci 2020;7(February):1–12. https://doi.org/10.3389/fvets.2020.00101.
[7] Krishnamurthy S, Deng B, del Rio R, Buchholz KR, Treeck M, Urban S, et al. Not a simple tether: Binding of Toxoplasma gondii AMA1 to RON2 during invasion protects AMA1 from rhomboid-mediated cleavage and leads to dephosphorylation of its cytosolic tail. MBio 2016;7(5). https://doi.org/10.1128/mBio.00754-16.

[8] Vieira FEG, Sasse JP, Minutti AF, Miura AC, de Barros LD, Cardim ST, et al. Toxoplasma gondii: prevalence and characterization of new genotypes in free-range chickens from south Brazil. Parasitol Res 2018;117(3):681–8.

[9] Slifko TR, Smith HV, Rose JB. Emerging parasite zoonoses associated with water and food. Int J Parasitol 2000;30(12-13):1379–93.

[10] Khan MB, Khan SNS, Rafiq K, Khan SNS, Attaullah S, Ali I. Molecular identification of Toxoplasma gondii in domesticated and broiler chickens (Gallus domesticus) that possibly augment the pool of human toxoplasmosis. PLoS One 2020; 15(4), doi: 10.1371/journal.pone.0232026.

[11] Zhao GW, et al. Detection of Toxoplasma gondii in free-range chickens in China based on circulating antigens and antibodies. Vet Parasitol 2012;185(2-4):72–7.

[12] Stelzer S, Basso W, Benavides Silván J, Ortega-Mora LM, Maksimov P, Gethmann J, et al. Toxoplasma gondii infection and toxoplasmosis in farm animals: Risk factors and economic impact. Food Waterborne Parasitol 2019;15:e00037.

[13] Tang X, Yin G, Qin M, Tao G, Suo J, Liu X, et al. Transgenic Eimeria tenella as a vaccine vehicle: Expressing TgSAG1 elicits protective immunity against Toxoplasma gondii infections in chickens and mice. Sci Rep Jul. 2016;6(1). https://doi.org/10.1038/srep29379.

[14] Zhao G-W, Wang S, Wang W, Zhang Z-C, Xie Q, Zhang M, et al. Type I strain of Toxoplasma gondii from chicken induced different immune responses with that from human, cat and swine in chicken. J Integr Agric 2015;14(5):956–65.

[15] Yu Z, et al. Toxoplasma gondii proteasome subunit alpha type 1 with chitosan: A promising alternative to traditional adjuvant. Pharmaceutics 2021; 13(5), May 2021, doi: 10.3390/pharmaceutics13050752.

[16] Chu KB, Quan FS. Advances in toxoplasma gondii vaccines: Current strategies and challenges for vaccine development. Vaccines Apr. 2021;9(5):413. https://doi.org/10.3390/vaccines9050413.

[17] Hajissa K, Zakaria R, Suppian R, Mohamed Z. Immunogenicity of multi-epitope vaccine candidate against Toxoplasma gondii infection in BALB/c mice. Iran J Parasitol 2018; 13(2): pp. 215–224, Accessed: Sep. 15, 2021. [Online]. Available: /pmc/articles/PMC6068360/.

[18] Dodangeh S, Fasihi-Ramandi M, Daryani A, Valadan R, Sarvi S. In silico analysis and expression of a novel chimeric antigen as a vaccine candidate against Toxoplasma gondii. Microb Pathog 2019;132:275–81.

[19] Ghaffari AD, Dalimi A, Ghaffarifar F, Pirestani M, Majidiani H. Immunoinformatic analysis of immunogenic b-and t-cell epitopes of mic4 protein to designing a vaccine candidate against toxoplasma gondii through an in-silico approach. Clin Exp Vaccine Res 2021;10(1):59–77. https://doi.org/10.7774/cevr.2021.10.1.59.

[20] Foroutan M, Ghaffarifar F, Sharifi Z, Dalimi A, Jorjani O. Rhoptry antigens as toxoplasma gondii vaccine target. Clin Exp Vaccine Res 2019;8(1):4–26. https://doi.org/10.7774/cevr.2019.8.1.4.

[21] Chen J, Li ZY, Petersen E, Huang SY, Zhou DH, Zhu XQ. DNA vaccination with genes encoding Toxoplasma gondii antigens ROP5 and GRA15 induces protective immunity against toxoplasmosis in Kunming mice. Expert Rev Vaccines Apr. 2015; 14(4):617–24. https://doi.org/10.1586/14760584.2015.1011133.

[22] Onile OS, Ojo GJ, Oyeyemi BF, Agbowuro GO, Fadahunsi AI. Development of multiepitope subunit protein vaccines against Toxoplasma gondii using an immunoinformatics approach. NAR Genom Bioinforma 2020;2(3):Sep. https://doi.org/10.1093/nargab/lqaa048.

[23] Dautu G, Munyaka B, Carmen G, Zhang G, Omata Y, Xuenan X, et al. Toxoplasma gondii: DNA vaccination with genes encoding antigens MIC2, M2AP, AMA1 and BAG1 and evaluation of their immunogenic potential. Exp Parasitol 2007;116(3): 273–82.

[24] Karimi M, et al. Construction of A Synthetic Gene Encoding the Multi-Epitope of Toxoplasma gondii and Demonstration of the Relevant Recombinant Protein Production: A Vaccine Candidate. Galen Med J 2020; 9: p. e1708, doi: 10.31661/gmj.v9i0.1708.

[25] Kim M-J, Lee S-H, Kang H-J, Chu K-B, Park H, Jin H, et al. Virus-like particle vaccine displaying Toxoplasma gondii apical membrane antigen 1 induces protection against T. gondii ME49 infection in mice. Microb Pathog 2020;142: 104090.

[26] Holec-gąsior L, Ferra B, Grążlewska W. Toxoplasma gondii tetravalent chimeric proteins as novel antigens for detection of specific immunoglobulin G in sera of small ruminants. Animals 2019;9(12):Dec. https://doi.org/10.3390/ani9121146.

[27] Ferra B, Holec-Gąsior L, Gatkowska J, Dziadek B, Dzitko K. Toxoplasma gondii recombinant antigen AMA1: Diagnostic utility of protein fragments for the detection of IgG and IgM antibodies. Pathogens 2020; 9(1), Jan. 2020, doi: 10.3390/pathogens9010043.

[28] Pastor-Fernández I, Kim S, Marugán-Hernández V, Soutter F, Tomley FM, Blake DP. Vaccination with transgenic Eimeria tenella expressing Eimeria maxima AMA1 and IMP1 confers partial protection against high-level E. maxima challenge in a broiler model of coccidiosis. Parasites Vectors 2020;13(1).

[29] Hanafiah M, Helmi TZ, Sutriana A, Priyowidodo D, Fihiruddin F. Cloning and expression of Toxoplasma gondii GRA-4 recombinant protein as a toxoplasmosis diagnostic kit candidate. Vet World Oct. 2020;13(10):2085. https://doi.org/10.14202/VETWORLD.2020.2085-2091.

[30] Yin G, Qin M, Liu X, Suo J, Suo X. Expression of Toxoplasma gondii dense granule protein7 (GRA7) in Eimeria tenella. Parasitol Res May 2013;112(5):2105–9. https://doi.org/10.1007/s00436-013-3307-5.

[31] Wang JL, et al. Immunization with Toxoplasma gondii GRA17 deletion mutant induces partial protection and survival in challenged mice. Front Immunol 2017; 8 (JUN):p. 730, doi: 10.3389/fimmu.2017.00730.

[32] Shaddel M, Ebrahimi M, Tabandeh MR. Bioinformatics analysis of single and multi-hybrid epitopes of GRA-1, GRA-4, GRA-6 and GRA-7 proteins to improve DNA vaccine design against Toxoplasma gondii. J Parasit Dis Jun. 2018;42(2):269–76. https://doi.org/10.1007/s12639-018-0996-9.

[33] Nielsen M, Lundegaard C, Lund O. Prediction of MHC class II binding affinity using SMM-align, a novel stabilization matrix alignment method. BMC Bioinf 2007;8(1).

[34] Adhikari UK, Rahman MM. Overlapping CD8 + and CD4 + T-cell epitopes identification for the progression of epitope-based peptide vaccine from nucleocapsid and glycoprotein of emerging Rift Valley fever virus using immunoinformatics approach. Infect Genet Evol 2017;56(September):75–91. https://doi.org/10.1016/j.meegid.2017.10.022.

[35] Kamthania M, Srivastava S, Desai M, Jain A, Shrivastav A, Sharma DK. Immunoinformatics Approach to Design T-cell Epitope-Based Vaccine Against Hendra Virus. Int J Pept Res Ther Dec. 2019;25(4):1627–37. https://doi.org/10.1007/s10989-018-09805-z.

[36] Mellet J, Tshabalala M, Agbedare O, Meyer P, Gray C, Pepper M. Human leukocyte antigen diversity and clinical application in South Africa. South African Med J 2021; 109(8b): pp. 29–34, Aug. 2019, Accessed: Jan. 22, 2021. [Online]. Available: https://scholar.google.com/scholar?q=Human leukocyte antigen diversity and clinical applications in South Africa.

[37] Thompson JD, Higgins DG, Gibson TJ. CLUSTAL W: Improving the sensitivity of progressive multiple sequence alignment through sequence weighting, position-specific gap penalties and weight matrix choice. Nucleic Acids Res Nov. 1994;22 (22):4673–80. https://doi.org/10.1093/nar/22.22.4673.

[38] Mugunthan SP, Harish MC. Multi-epitope-Based Vaccine Designed by Targeting Cytoadherence Proteins of Mycoplasma gallisepticum. ACS Omega 2021;6(21): 13742–55. https://doi.org/10.1021/acsomega.1c01032.

[39] Andreatta M, Nielsen M. Gapped sequence alignment using artificial neural networks: application to the MHC class I system. Bioinformatics 2016; 32(4): pp. 511–517, Feb. 2016, Accessed: Jan. 22, 2021. [Online]. Available: https://academic.oup.com/bioinformatics/article-abstract/32/4/511/1744469.

[40] Higgs R, Cormican P, Cahalane S, Allan B, Lloyd AT, Meade K, et al. Induction of a Novel Chicken Toll-Like Receptor following Salmonella enterica Serovar Typhimurium Infection. Infect Immun 2006;74(3):1692–8.

[41] Bui HH, Sidney J, Dinh K, Southwood S, Newman MJ, Sette A. Predicting population coverage of T-cell epitope-based diagnostics and vaccines. BMC Bioinf Mar. 2006;7. https://doi.org/10.1186/1471-2105-7-153.

[42] Dimitrov I, Flower DR, Doytchinova I. AllerTOP - a server for in silico prediction of allergens. BMC Bioinf 2013;14(S6).

[43] Dimitrov I, Naneva L, Doytchinova I, Bangov I. AllergenFP: allergenicity prediction by descriptor fingerprints. Bioinformatics 2014; 30(6): pp. 846–851, doi: 10.1093/BIOINFORMATICS/BTT619.

[44] Pandey RK, Kumbhar BV, Srivastava S, Malik R, Sundar S, Kunwar A, et al. Febrifugine analogues as Leishmania donovani trypanothione reductase inhibitors: binding energy analysis assisted by molecular docking, ADMET and molecular dynamics simulation. J Biomol Struct Dyn 2017;35(1):141–58.

[45] Chauhan V, Rungta T, Goyal K, Singh MP. Designing a multi-epitope based vaccine to combat Kaposi Sarcoma utilizing immunoinformatics approach. Sci. Rep. 2019; 9(1), doi: 10.1038/s41598-019-39299-8.

[46] Heo L, Park H, Seok C. GalaxyRefine: Protein structure refinement driven by side-chain repacking. Nucleic Acids Res 2013; 41(Web Server issue), p. W384, doi: 10.1093/NAR/GKT458.

[47] Ko J, Park H, Seok C. GalaxyTBM: Template-based modeling by building a reliable core and refining unreliable local regions. BMC Bioinf 2012;13(1):1–8. https://doi.org/10.1186/1471-2105-13-198.

[48] Laskowski RA, MacArthur MW, Moss DS, Thornton JM. PROCHECK: a program to check the stereochemical quality of protein structures. J Appl Crystallogr 1993;26 (2):283–91. https://doi.org/10.1107/S0021889892009944.

[49] S. de Vries, J. Rey, C. Schindler, M. Zacharias, P. Tuffery, The pepATTRACT web server for blind, large-scale peptide–protein docking, vol. 45, no. 1, pp. 361–364, Jul. 2017, Accessed: Jan. 22, 2021. [Online]. Available: https://academic.oup.com/nar/article-abstract/45/W1/W361/3782603.

[50] Adeleke VT, Adeniyi AA, Adeleke MA, Okpeku M, Lokhat D. The design of multiepitope vaccines from plasmids of diarrheagenic Escherichia coli against diarrhoea infection: Immunoinformatics approach. Infect Genet Evol 2021;91: 104803.

[51] Humphrey W, Dalke A, Schulten K. VMD: Visual molecular dynamics. J Mol Graph 1996;14(1):33–8. https://doi.org/10.1016/0263-7855(96)00018-5.

[52] Pettersen EF, Goddard TD, Huang CC, Couch GS, Greenblatt DM, Meng EC, et al. UCSF Chimera - A visualization system for exploratory research and analysis. J Comput Chem 2004;25(13):1605–12.

[53] Case DA, et al. Amber 14. San Francisco: University Of California; 2014.

[54] Maier JA, Martinez C, Kasavajhala K, Wickstrom L, Hauser KE, Simmerling C. ff14SB: Improving the Accuracy of Protein Side Chain and Backbone Parameters from ff99SB. J Chem Theory Comput 2015;11(8):3696–713. https://doi.org/10.1021/acs.jctc.5b00255.

[55] Ojha R, Gupta N, Naik B, Singh S, Verma VK, Prusty D, et al. High throughput and comprehensive approach to develop multiepitope vaccine against minacious COVID-19. Eur J Pharm Sci 2020;151:105375.

[56] Khodadadi M, Ghaffarifar F, Dalimi A, Ahmadpour E. Immunogenicity of in-silico designed multi-epitope DNA vaccine encoding SAG1, SAG3 and SAG5 of Toxoplasma gondii adjuvanted with CpG-ODN against acute toxoplasmosis in BALB/c mice. Acta Trop 2021;216:105836.

[57] Yadav S, Prakash J, Shukla H, Das KC, Tripathi T, Dubey VK. Design of a multi-epitope subunit vaccine for immune-protection against Leishmania parasite. Pathog Glob Health 2020;114(8):471–81. https://doi.org/10.1080/20477724.2020.1842976.

[58] Shey RA, Ghogomu SM, Esoh KK, Nebangwa ND, Shintouo CM, Nongley NF, et al. In-silico design of a multi-epitope vaccine candidate against onchocerciasis and

related filarial diseases. Sci Rep 2019;9(1). https://doi.org/10.1038/s41598-019-40833-x.
[59] Foroutan M, Ghaffarifar F, Sharifi Z, Dalimi A. Vaccination with a novel multi-epitope ROP8 DNA vaccine against acute Toxoplasma gondii infection induces strong B and T cell responses in mice. Comp Immunol Microbiol Infect Dis 2020;69:101413.
[60] R.A. Strikas, A.C. Mawle, L.K. Pickering, W.A. Orenstein, Active Immunization, in: Principles and Practice of Pediatric Infectious Diseases, Elsevier, 2018, pp. 43-71.e4.
[61] Zhang Lu, Wang W, Wang S. Effect of vaccine administration modality on immunogenicity and efficacy. Expert Rev Vaccines 2015;14(11):1509–23.
[62] Forouharmehr A, Banan A, Mousavi SM, Jaydari A. Development of a Novel Multi-Epitope Vaccine Candidate against Streptococcus Iniae Infection in Fish: An Immunoinformatics Study. Arch Razi Inst 2022;77(1):35–46. https://doi.org/10.22092/ARI.2021.353377.1601.
[63] Singh A, Thakur M, Sharma LK, Chandra K. Designing a multi-epitope peptide based vaccine against SARS-CoV-2. Sci Rep 2020;10(1):16219. https://doi.org/10.1038/s41598-020-73371-y.
[64] Verhelst D, De Craeye S, Entrican G, Dorny P, Cox E. Parasite distribution and associated immune response during the acute phase of toxoplasma gondii infection in sheep. BMC Vet Res 2014;10(1):1–12. https://doi.org/10.1186/s12917-014-0293-5.
[65] Cong H, Yuan Q, Zhao Q, Zhao L, Yin H, Zhou H, et al. Comparative efficacy of a multi-epitope DNA vaccine via intranasal, peroral, and intramuscular delivery against lethal Toxoplasma gondii infection in mice. Parasites Vectors 2014;7(1):145.
[66] Sasai M, Yamamoto M. Innate, adaptive, and cell-autonomous immunity against Toxoplasma gondii infection. Exp Mol Med 2019;51(12):1–10.
[67] Fatoba AJ, Adeleke VT, Maharaj L, Okpeku M, Adeniyi AA, Adeleke MA. Immunoinformatics Design of Multiepitope Vaccine Against Enterococcus faecium Infection. Int J Pept Res Ther 2021;27(4):2183–98. https://doi.org/10.1007/s10989-021-10245-5.
[68] Naeimi R, Bahmani A, Afshar S. Investigating the role of peptides in effective therapies against cancer. Cancer Cell Int 2022;22(1):1–10. https://doi.org/10.1186/S12935-022-02553-7/FIGURES/2.